Rev. Colomb. Quím., 2012, **41**(1): 133-157

De novo DESIGN AND SYNTHESIS OF AN ICE-BINDING, DENDRIMERIC, POLYPEPTIDE BASED ON INSECT ANTIFREEZE PROTEINS

SÍNTESIS Y DISEÑO De novo DE UN POLIPÉPTIDO DENDRÍMERO CON UNIÓN AL HIELO BASADO EN LAS PROTEINAS ANTICONGELANTES DE INSECTOS

SÍNTESE E DESENHO DE NOVO DE UM POLIPEPTÍDEOS DENDRÍMERO COM UNIÃO AO GELO BASEADO NAS PROTEÍNAS ANTICONGELANTES DE INSETOS

Ricardo Vera-Bravo[1,4], Andrew J Scotter[2], Peter L Davies[2] and Luis H Blanco[3]

Recibido: 01/12/11 – Aceptado: 23/04/12

ABSTRACT

A new strategy is presented for the design and synthesis of peptides that exhibit ice-binding and antifreeze activity. A pennant-type dendrimer polypeptide scaffold combining an α-helical backbone with four short β-strand branches was synthesized in solid phase using Fmoc chemistry in a divergent approach. The 51-residue dendrimer was characterized by reverse phase high performance liquid chromatography, mass spectrometry and circular dichroism. Each β-strand branch contained three overlapping TXT amino acid repeats, an ice-binding motif found in the ice-binding face of the spruce budworm (*Choristoneura fumiferana*) and beetle (*Tenebrio molitor*) antifreeze proteins. Ice crystals in the presence of the polypeptide monomer displayed flat, hexagonal plate morphology, similar to that produced by weakly active antifreeze proteins. An oxidized dimeric form of the dendrimer polypeptide also produced flat hexagonal ice crystals and was capable of inhibiting ice crystal growth upon temperature reduction, a phenomenon termed thermal hysteresis, a defining property of antifreeze proteins. Linkage of the pennant-type dendrimer to a tri-functional cascade-type polypeptide produced a trimeric macromolecule that gave flat hexagonal ice crystals with higher thermal hysteresis activity than the dimer or monomer and an ice crystal

1 Departamento de Química, Pontificia Universidad Javeriana, Bogotá, D.C., Colombia

2 Department of Biochemistry, Queen's University, Kingston, Ontario, Canada, K7L3N6

3 Universidad Nacional de Colombia, sede Bogotá, Facultad de Ciencias, Departamento de Química, Laboratorio de Investigaciones Básicas. Av Cra 30 45-03- Bogotá D.C., Código Postal 111321 - Colombia.

4 verar@javeriana.edu.co

burst pattern similar to that produced by samples containing insect antifreeze proteins. This macromolecule was also capable of inhibiting ice recrystallization.

Keywords: Antifreeze protein, dendrimer, synthetic polypeptide, thermal hysteresis, ice recrystallization inhibition

RESUMEN

Una nueva estrategia se presenta para el diseño y síntesis de péptidos que se unen al hielo y evidencian actividad anticongelante. Un polipéptido dendrímero del tipo banderín, que combina en su estructura un núcleo α-hélice con cuatro ramificaciones cortas de hojas β, se sintetizó en fase sólida utilizando la química Fmoc con una estrategia divergente. El dendrímero de 51 residuos se caracterizó por cromatografía líquida de alta resolución, espectrometría de masas y dicroísmo circular. Cada ramificación de hoja β contiene tres repeticiones de los motivos de aminoácidos TXT sobrelapados, un motivo de unión al hielo presente en la cara de unión de las proteínas anticongelantes del gusano de brotes de abeto (*Choristoneura fumiferana*) y en el escarabajo (*Tenebrio molitor*). Los cristales de hielo en presencia del polipéptido monomérico presentan una morfología hexagonal plana, similar a la producida por las proteínas anticongelantes con una débil actividad. Un dímero oxidado del polipéptido también produce cristales de hielo hexagonales planos que fueron capaces de inhibir el crecimiento de los cristales de hielo a medida que se disminuía la temperatura, un fenómeno conocido como histéresis térmica, esto es, una propiedad que define las proteínas anticongelantes. La vinculación del dendrímero tipo banderín a un polipéptido tipo cascada trifuncional produjo una macromolécula trimérica que generó cristales de hielo hexagonales planos con una mayor actividad de histéresis térmica que los dímeros y los monómeros y un patrón de estallido del cristal de hielo muy similar al producido por las muestras que contienen proteínas anticongelantes de insectos. Estas moléculas además fueron capaces de inhibir la recristianización del hielo.

Palabras clave: proteína anticongelante, dendrímero, polipéptido sintético, histéresis térmica, inhibición de la recristianización del hielo.

RESUMO

Uma nova estratégia é apresentada para o desenho e síntese de peptídeos que se unem ao gelo e apresentam atividade anticongelante. Um polipeptídeo dendrímero do tipo pennant que combina em sua estrutura um núcleo α-hélice com quatro ramificações curtas de folhas β foi sintetizado em fase sólida utilizando a química Fmoc com uma estratégia divergente. O dendrímero de 51 resíduos foi caracterizado por cromatografia líquida de alta resolução, espectrometria de massas e dicroísmo circular. Cada ramificação de folha β contém três repetições dos motivos de aminoácidos TXT sobrepostos, um motivo de união ao gelo presente na cara de união das proteínas anticongelantes do verme de Choristoneura fumiferana e no escaravelho (Tenebrio molitor). Os cristais de gelo, em presença do polipeptídeo monomérico, apresentam uma morfologia hexagonal plana, similar à produzida pelas proteínas anticongelantes com uma atividade fraca. Um dímero

oxidado do polipeptídeo também produz cristais de gelo hexagonais planos e foram capazes de inibir o crescimento dos cristais de gelo à medida que a temperatura diminuia, um fenômeno conhecido como histerese térmica una propriedade que define as proteínas anticongelantes. A vinculação do dendrímero tipo pennant a um polipeptídeo tipo cascata trifuncional produziu uma macromolécula trimérica que gerou cristais de gelo hexagonais planos com uma maior atividade de histerese térmica que os dímeros e os monómeros e um padrão de estouro do cristal de gelo muito similar ao produzido pelas amostras que contêm proteínas anticongelantes de insetos. Estas moléculas, aliás, foram capazes de inibir a recristalização do gelo.

Palavras-chave*:* proteína anticongelante, dendrímero, polipeptídeo sintético, histerese térmica, inibição da recristalização do gelo.

INTRODUCTION

Dendrimers are a group of branched macromolecular compounds with varied physicochemical properties, composition, molecular weight and structures that are finding use in several fields of research (1, 2). Depending on the distribution of branches, dendrimers can be classified as cascade, pennant or radial-types (3, 4). In general, dendrimers consist of three parts: a central core, branching units and functional groups at the ends of the branches. Peptide dendrimers that are synthesized without a core and that grow in one direction are usually termed dendrons (1, 2, 5), but this distinction is not made here.

The synthesis of dendrimer polypeptides allows for the generation of multivalent macromolecules (with several copies of a functionally active sequence of interest) that are able to create multiple bonds or simultaneous interactions with receptor molecules thereby increasing the affinity and specificity of the interaction. Synthesis of such multivalent macromolecules can be carried out by either a direct approach (a divergent strategy) using consecutive peptide synthesis steps in solid phase or by an indirect approach using condensation methods (a convergent strategy) (6, 7). Lysine is the amino acid most commonly used to produce branching points in dendrimers due to the presence of two spatially separated reactive amino groups (-NH_2) within the same molecule.

Depending on the type of protection group chemistry employed on the α- and ε-amino groups there are two possibilities for dendrimer synthesis. When the two amino groups are protected by the same protecting group, a parallel addition of the same branch and/or functional group ensues upon deprotection at both amino groups to produce two similar arms. If the α- and ε-amino groups are protected by different groups, different deprotection methods are used so that each amino group can couple with different branches/functional groups in a selective way at specific times during the synthesis of the dendrimer (2, 6).

The field of dendron and dendrimer synthesis and their applications has become increasingly important in recent years. Cascade-type dendrimers, including the generation of multiple antigenic peptides (MAP) (1), have been widely

studied and several potential biotechnological and medical applications have been proposed (8-11). To date, there have been few reports of synthetic pennant-type dendrimers except for *de novo* protein synthesis using the concept of template-assembled synthetic proteins (7, 12-15). Generally, pennant-type peptides have a backbone sequence that has regularly spaced lysine residues from which the molecules that form the branches are synthesized or bonded (3, 16).

Many proteins show multiple, simultaneous interactions with their biological targets through the presence of several short binding motifs that result in a higher affinity interaction, a phenomenon termed avidity. The antifreeze proteins (AFP) of spruce budworm (*Cf*AFP) and *Tenebrio molitor* (*Tm*AFP) use an array of threonines on one face of a highly ordered, disulfide-bond stabilized, β-helix to bind to the surface of ice crystals and inhibit their growth through an adsorption-inhibition mechanism (17). The threonine residues on the ice-binding face of the AFP form two rows that closely match the spacing of water molecules on the primary prism plane and basal plane of an ice crystal (18-23). The X residue in the TXT repeat is an amino acid in a short β-strand that points into the core of the protein. It is flanked by two threonine side chains pointing out of the short β-strand. Most isoforms of the insect AFPs have five or six TXT motifs. The presence of additional TXT motifs, either in naturally occurring longer isoforms (23) or those that have been recombinantly engineered (24) correlates with higher antifreeze activity.

Using *Cf*AFP and *Tm*AFP for guidance, a pennant-type dendrimeric polypeptide was designed and synthesized as shown in Figures 1 and 2. The peptide has an α-helical backbone that contains four lysine residues as branching points. These branching points were distributed so that they would be arrayed on one side of the α-helical backbone, see Figure 1b. Each branching point was modified with a peptide containing TXT repeats creating a scaffold of four TXTXTXT sequences, mimicking and extending the ice-binding face of *Cf*AFP and *Tm*AFP. The pennant-type dendrimer also contains a C-terminal cysteine residue that upon oxidation can form a disulfide bond with a second dendrimer allowing for the formation of a dendrimer dimer with eight TXTXTXT motifs, see Figure 2b. The oxidation of the dendrimer monomer in the presence of a short cascade-type dendrimer that has three terminal cysteine residues has the potential to make a trimeric dendrimer macromolecule formed around a cascade-type hub. This polymer would contain twelve TXTXTXT repeats, see Figure 2b. These TXT branches may adopt β-strand secondary structure similar to insect AFP TXT motifs and the glycine residues linking them to the backbone were built in to allow for branch flexibility and their optimal arrangement on the surface of an ice crystal.

The pennant-type dendrimer and its polymers displayed ice-binding properties, ice crystal morphology and ice crystal burst pattern akin to *Cf*AFP and *Tm*AFP. Thermal hysteresis activity and ice-recrystalization inhibition activity have also been demonstrated for the oxidized dimer and trimer forms of the den-

drimer illustrating that it is possible to synthesize pennant-type dendrimers with antifreeze protein-like activity.

MATERIALS AND METHODS

Peptide synthesis

The pennant-type polypeptides were manually synthesized in a divergent strategy, on a solid support of Novasyn TGR resin (100 mg), using Novabiochem (USA) Nα –Fmoc-L- amino acids, Merck analytical solvents and good manufacture practice norms. For the coupling reactions, and depending on the grade of difficulty, three protocols of coupling cycles were used with the following combinations of activators and catalysts: 1) Nα–Fmoc-L- amino acids/ N,N'-dicyclohexylcarbodiimide (DCC)/ N-Hydroxybenzotriazole (HOBt); in 1:1:1 ratio in Dimethylformamide (DMF), 2) Nα–Fmoc-L- amino acids/ 2-(1H-benzotriazole-1-yl)-1,1,3,3-tetramethyluronium tetrafluoroborate (TBTU)/ HOBt/ N,N-diisopropylethylamine (DIPEA); in (1:1:1:2.5) ratio, in N-methyl-2-pyrrolidine (NMP), 3) Nα–Fmoc-L- amino acids/ benzotriazole-1-yl-N-oxy-tris-pyrrolidino-phosphonium hexafluorophosphate (PyBOP)/ HOBt/ DIPEA in (1:1:1:2.5) ratio, in DMF-NMP (1:1). The α-amino Fmoc protecting group was removed using 25 % piperidine in DMF, and the deprotection and the coupling reaction were monitored using the Kaiser test (25). A four-fold excess of amino acid with respect to the level of resin substitution were used with coupling times between 2 and 4 h. A kaiser´s test is then performed to confirm that complete coupling has occurred on all the free amines on the resin. Once the synthesis ended, the peptide was cleaved from the resin and the protecting groups from the side chains by treatment with trifluoroacetic acid (TFA), triisopropylsilane (TIS), water and ethanedithiol in a 93:2:2.5:2.5 ratio for 4 h at room temperature. The cleaved peptide was precipitated with ice-cold diethyl ether, extracted with 5 % acetic acid and lyophilized. The peptide was analyzed by RP-HPLC on a Lichro-CART RP-18 (Merck) C-18 column (125 x 5 mm) using a linear gradient of 0-70 % acetonitrile (0.05 % TFA) in water (0.05 % TFA) over 45 min at a flow rate of 1 mL/ min with UV detection at 210 nm. The molecular weight of the peptides was determined by MALDI-TOF (Autoflex, Bruker) mass spectrometry, using α-cyano-4-hydroxy-cinnamic acid (CCA) as the matrix.

Acetylation of the amino groups

The amino group that did not react during the coupling (i.e. the N-terminal amino group of K^1) was blocked by means of two treatments with acetic anhydride, pyridine and DMF in a 1:1:1 ratio for 30 min, followed by Kaiser´s test for completion of the reaction. Subsequently, backbone peptide synthesis continued until complete. The Fmoc group of the terminal amino residue was removed with 25 % piperidine in DMF, after which the amino group was acetylated to block its reactivity during addition of the branches.

Branch Preparation

Diprotected N(α), N(ε) lysine residues were used as branching points. Protection of these four backbone lysine residues

(K^4, K^8, K^{11}, K^{15}) was achieved by addition of Novabiochem Nα-Fmoc-L-Lys(ivDde)-OH (26). Once the synthesis of the backbone was complete and the N-terminus of the peptide was acetylated, the protecting group 1-(4,4-dimethyl-2,6-dioxocyclohex-1-ylidene)-ethyl (ivDde) was removed from the side chain by three treatments with 2 % hydrazine in DMF for 5 min, followed by Kaiser´s test to confirm deprotection. A coupling cycle with Nα–Fmoc-L-amino acids/ TBTU/ HOBt/ DIPEA at a 1:1:1:2.5 ratio in NMP was carried out to couple the first residue to each branch point. A kaiser´s test is then performed to confirm that complete coupling has occurred on all the free amines on the resin. The subsequent amino acids along the branches were coupled according to the protocols of synthesis previously described (1, 2 and 3). The sequence of the complete monomeric pennant-type dendrimer was:

$(TLTTTITG)_4$AcKAA**K**KTA**K**AA**K**AT A**K**EAKC.

Cascade polypeptide synthesis

For the cascade type peptide synthesis, Novabiochem Nα-Fmoc-L-Lys(Fmoc)-OH was added to protect the α- and ε-amino groups of the lysine residues using 25 % piperidine in DMF, followed by Kaiser´s test. The subsequent coupling steps were carried out in the usual manner, followed by Kaiser´s test. The sequence of the complete cascade-type dendrimer was $(CKIKL)_2$**K**LKIKC.

Peptide oxidation

Cysteine residues were incorporated at the amino terminus and/or carboxy terminus of the polypeptides to allow for the formation of disulfide-bonded dimers and larger macromolecules via oxidation of the peptides (Figure 2). The peptides were dissolved in deionized water; the pH was adjusted to 7.5 with ammonium bicarbonate (0.1 M), and the peptides were subjected to oxidative conditions using a constant oxygen flow for 48 h. The pennant-type peptide was dissolved at 4 mg/mL to form the dimer. For the preparation of the polymeric macromolecule a ratio 1:3 of the cascade-type polypeptide with respect to the pennant-type polypeptide was used.

Secondary structure analysis

Predictions of the secondary structure based on the antifreeze peptide primary sequence were determined using the algorithms GOR1, GOR3, MLRC and PHD (27).

Circular dichroism (CD) studies

CD spectra were collected using a JASCO J810 (Jasco, Easton, MD) spectropolarimeter equipped with a thermostatic NESLAB RTE7 water bath using a 1 cm path length quartz cell. Analyses were performed using a 5 μM concentration of peptide in 30 % trifluoroethanol TFE/ water mixture. The spectra between 190 nm and 260 nm were recorded at -1.5 and 18 ºC with a band width of 0.2 nm and a scanning speed of 10 nm/min. The CD data are expressed as mean residue Molar ellipticity [θ], (deg cm^2 $dmol^{-1}$) and are the average of three datasets.

Thermal hysteresis assay

Thermal hysteresis is defined as the difference between the melting point and

the non-equilibrium freezing point of a solution measured in centigrade degrees (C°). The thermal hysteresis activity of the polypeptides was measured as described by Chakrabartty and Hew (28), using a nanolitre osmometer (Clifton Technical Physics, Hartford, NY). All samples were buffered in 0.1 M ammonium bicarbonate (NH_4HCO_3), 9 % v/v acetic acid and 2 % v/v acetonitrile. The freezing point is determined when the growth of the crystal is equal to or greater than 2 μm/s. Digital images and movies of each sample's ice crystal morphology and ice crystal burst were recorded on a Nikon Coolpix 4500 digital camera mounted on a Leitz Dialux 22 microscope at 320 x magnification. The assays were carried out in triplicate under identical conditions: the reported values are the average of the three separate samples. Thermal hysteresis activity was determined using a nanolitre osmometer with a cooling rate of 40 mOsm/min (1000 mOsm = 1.86 ºC). Buffer controls and positive controls using recombinant *Cf*AFP (0.075 mg/mL) were also collected. The thermal hysteresis activity at various pH values was also determined. The sample pH was adjusted using acetic acid at a concentration of dendrimer polypeptide of 10 mg/mL.

Recrystallization inhibition assay

For this assay the improved method of recrystallization inhibition in capillaries was used (29). Samples of the dendrimer polymer (10 mg/mL) were placed inside 10 µl glass micro-capillaries (51 mm long and 1 mm diameter) in addition to buffer samples (same buffer as TH assays) and *Cf*AFP positive controls (0.075 mg/mL). The tubes were sealed with vacuum grease, aligned and held with clamps. The samples were rapidly cooled in 40 % ethylene glycol at -25 ºC for 15 min. Frozen samples were then placed in a jacketed container filled with -25 ºC 40 % ethylene glycol and were slowly warmed to -6 ºC using a programmable temperature controlled circulating water bath. The crystal size was followed for 18 h using a microscope, illuminated from below fitted with cross-polarizing filters.

RESULTS

Peptide design

A 51-residue (19 + 4 x 8) non-mimetic peptide was synthesized that combines an α-helix backbone with four β-strand branches based on the TXT ice-binding motif of *Cf*AFP and *Tm*AFP. Amino acids with a high propensity to form α-helices (Ala, Lys, Glu) were chosen for the backbone sequence (30-31). To compensate for the loss of charge on the branching lysine residues (K^4, K^8, K^{11}, K^{15}) and the hydrophobic branching sequences, charged residues like K^1, K^5, K^{18} and E^{16} were incorporated to improve the solubility of the polypeptide. The residues K^5 and E^{16} were introduced to encourage formation an inter-α-helical salt bridge between two separate antiparallel polypeptides. Of the 15 TXT motifs present in several *Cf*AFP isoforms (22), TIT, TTT and TLT were selected because the X amino acids (I, T and L) have a high intrinsic propensity to form and stabilize β-strands. Diagrams summarizing the design, synthesis and predicted secondary structure of the polypeptide design are shown in Figures 1 and 2. Various secondary structure prediction algorithms

were used including GOR 1 with an accuracy of correct residue assignment between 55 and 63% (32), GOR 3 with accuracy between 63 and 69% (33), HNNC (34), MLRC (35) and PHD, an artificial neuronal network, with 74% accuracy (36). The consensus secondary structure prediction results are shown in Figure 1b. A helical wheel structure representation of the backbone sequence is also presented in Figure 1b highlighting the position of the amino acids and the orientation of the branching lysine residues.

Peptide synthesis

A conventional approach of successive synthetic steps was used for the preparation of the dendrimeric polypeptides; this involved the progressive addition of Nα-Fmoc protected amino acids to a deprotected Nα-amino acid belonging to the

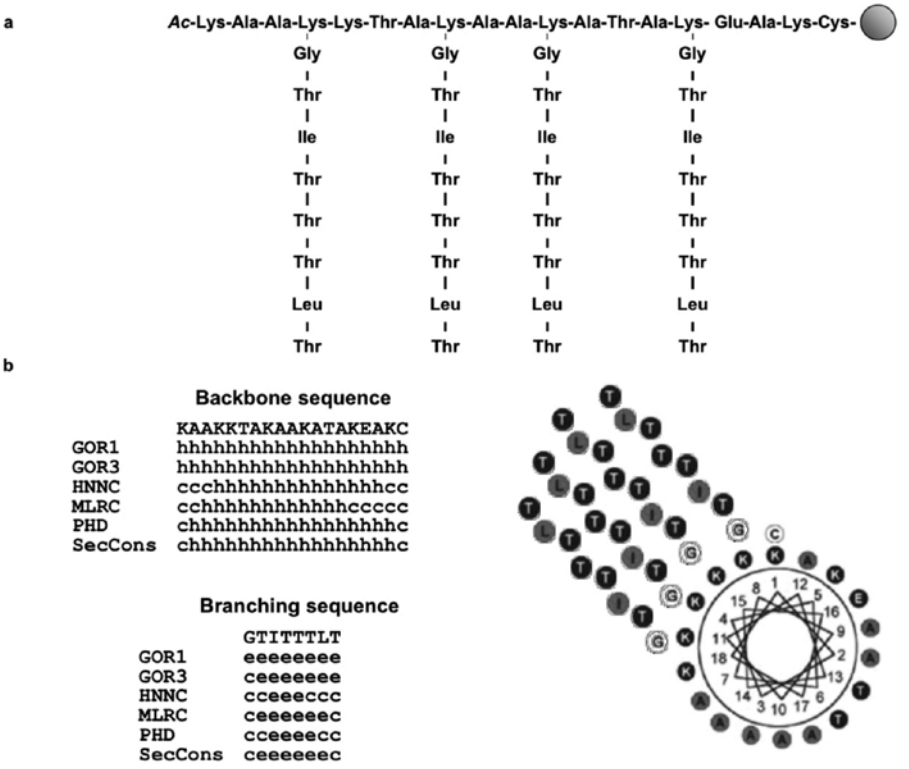

Figure 1. Design, structural prediction and synthesis of the pennant-type dendrimer polypeptide. **a.** Amino acid sequence and placement of the 4 branching points at K^4, K^8, K^{11}, K^{15}, Ac represents the acetylation of the α-amino group. **b.** Prediction of the secondary structure using the algorithms GOR1, GOR3, HNNC, MLRC, PHD (32-36) for the backbone as well as the branches and helical wheel representation of the backbone. Key = h (alpha helix structure), e (extended strand structure) and c (random coil).

growing peptide sequence anchored to a solid support. The use of a Nα-, Nε- diprotected L-Lysine residue with specific protective groups (Nα–Fmoc and Nε-ivDde) allowed for the addition of branch peptides at specific points (K^4, K^8, K^{11}, K^{15}) (3-4, 37). Using the methods of divergent solid-phase synthesis and Fmoc chemistry the peptides were obtained as summarized in Figure 2a. As the structural complexity of the peptide grew during its preparation some difficulties were encountered. One of them was incomplete removal of the Nα-Fmoc group of the amino acids during extension of the branches. For this purpose the percent of piperidine was increased to 40 % with the addition of 1 % of Triton X-100 in DMF. Due to the hydrophobic character of the branches there were some difficulties completing the coupling. These were eased by using different coupling cycles (see the Experimental Methods section) together with incubation at between 40 and 50 ˚C. In addition, the use of ultrasonic vibration and the addition of 1 %

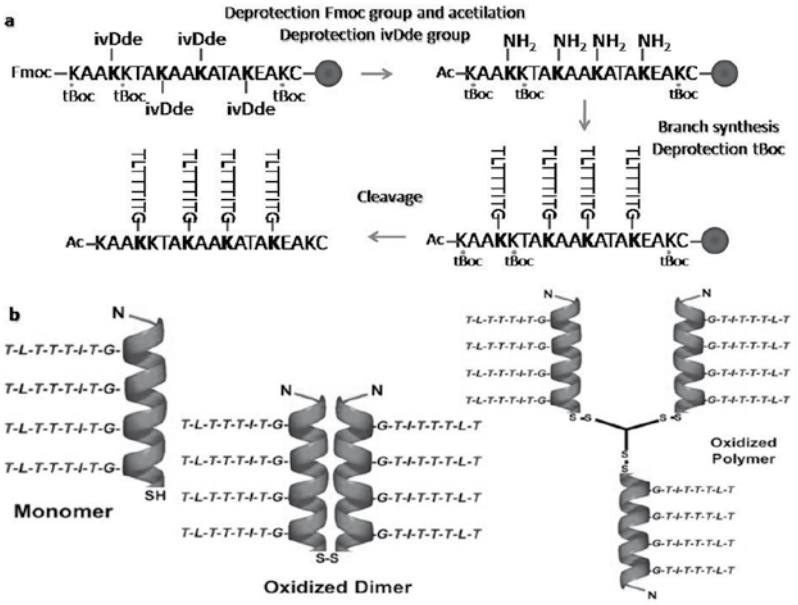

Figure 2. a. Schematic representation of the peptide synthesis. The backbone of the polypeptide was successively synthesized on TGR resin, then the Fmoc protecting group of K^1 was removed and the free amide group was acetylated. The ε-amino ivDde protective groups of K^4, K^8, K^{11} and K^{15} residues were then removed so synthesis of the branches could begin. Upon completion of branch synthesis the branch C-terminal amide groups were removed in addition to the remaining backbone amino acids' protective groups. The polypeptide was cleaved from the resin by treatment with TFA/TIS/EDT/H_2O. The steps requiring most attention were the deprotection of the K^4, K^8, K^{11} and K^{15} residues and the later coupling of the first residue of each branch. **b.** Schematic representation of the monomer, oxidized dendrimer dimer and oxidized polymer comprised of three pennant-type monomers and a cascade-type dendrimer hub.

Triton X-100 allowed for a better presentation of the carboxylic group of the amino acid in the peptide and better accessibility during the time of coupling, due to the unfolding of the peptide chain.

The complete 51-residue dendrimer polypeptide $(TLTTTITG)_4$AcKAA**K**KT A**K**AA**K**ATA**K**EAKC, was characterized using MALDI TOF mass spectrometry and RP HPLC as shown in Figures 3a and 3b. The chromatography profile shows a peak with a retention time of 24.48 min in a linear gradient of 0-70 % acetonitrile (0.05 % TFA) in water (0.05 % TFA). The mass measured by MALDI TOF mass spectrometry agreed with that calculated (5123 Da) for this Ala-and Thr-rich sequence. The cascade-type dendrimer linker $(CKIKL)_2$**K**LKIKC is a 16-residue peptide with a characterized mass of 1904 Da and a retention time of 22.8 min (Figure 3c and 3d). As a result of the hydrophobic character of the polypeptide, aqueous solubility of the pennant-type dendrimer was quite low. It was necessary to first dissolve the peptide in an organic solvent for the analysis. For chromatography, a mixture of the TFA/ acetonitrile (ACN) was used; for CD, the addition of TFE was adequate; for thermal hysteresis assays a mixture of acetic acid and ACN was used, followed by drop by drop addition of ammonium bicarbonate (0.1 M, pH 7.9).

CD spectra

The CD spectra generated for the pennant-type dendrimer peptide are consistent with a combination of secondary structures derived mainly from α-helix and β-strands with a small fraction of random coil, as shown in Figure 4. The characteristic α-helix CD spectrum has a maximum at 190 nm (π-π* transitions), and two minima, one at 208 nm (π-π* transitions), the other at 222 nm (n-π* transitions). In the spectrum obtained at 18 ºC the minima for the dendrimer polypeptide are at 205 and 220 nm and the 205 nm band shows a slightly higher intensity than the band at 220 nm, which is in agreement with previous findings

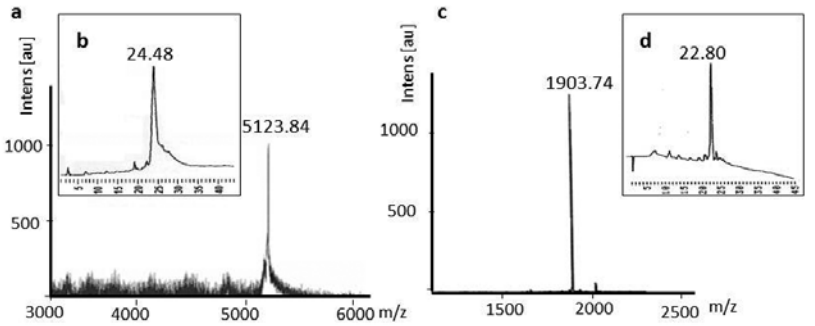

Figure 3. Characterization of the dendrimeric peptides that were synthesized. **a**. Mass spectrum by MALDI TOF and **b**. RP-HPLC profile of the pennant-type antifreeze polypeptide $(TLTTITG)_4$ AcKAA**K**KTA**K**AA**K**ATA**K**EAKC. **c**. Mass spectrum MALDI TOF and **d**. RP-HPLC profile of the cascade-type polypeptide $(CKIKL)_2$**K**LKIKC where **K** represents the branching lysine point and *Ac* the acetylated lysine α-amino group.

for proteins that show a transition from a random coil to a combination of α-helix and β-strand (38).

Two additional spectra were taken at 5 and -1 ºC, see Figure 4, to determine the behavior of the polypeptide structure at the low temperatures required for its function of ice binding. An increase in the intensity of the maxima at 190 nm together with a displacement of the negative minimum at 207 nm for 5 ºC and at 208 nm at -1 ºC, are observed. These results confirm the presence of α-helical structural elements in higher proportion and less β-strands character at low temperatures, which is in agreement with the secondary structure predictions and with previous studies on structured peptides, using various solvents (39, 40). In aqueous solution, hydrophobic peptides tend to be insoluble and organic solvents are required to dissolve them. An aqueous solution of 30 % trifluoroethanol TFE/ water allowed the dissolution of the dendrimer polypeptide and subsequent analysis to determine the folding of the peptide. At this concentration of TFE, stabilization of peptides with a clear tendency to form secondary structures occurs (41-43). Figure 4 also shows the CD spectrum of the antifreeze peptide for the oxidized polymer (comprised of three pennant-type and one cascade-type dendrimers). It shows a decrease in α-helical tendency and a greater pres-

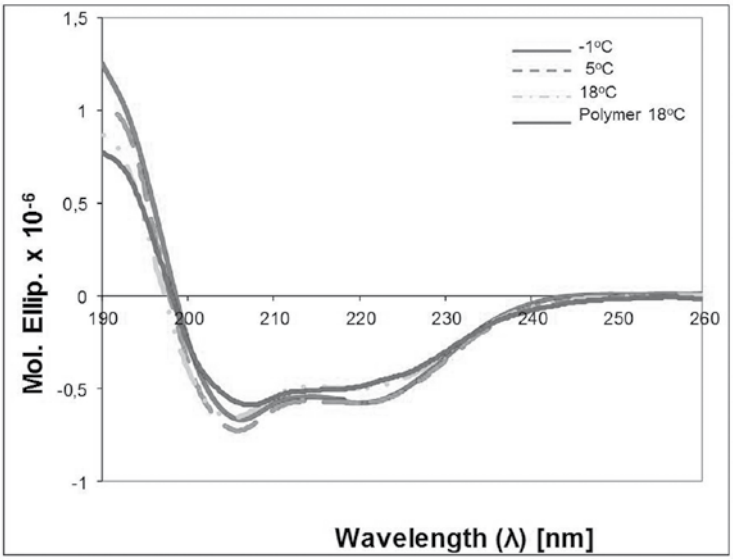

Figure 4. Circular dichroism spectra of the pennant-type synthetic polypeptide (50 μM) in 30% TFE, as a function of temperature. The continuous red line, the dashed green line, and the dash-dot-dash orange line represent data collected at -1ºC, 5 ºC, and 18 ºC, respectively (all at pH 4). The continuous blue line corresponds to the pennant-type polypeptide dimer formed after oxidation of the pennant-type monomer with the cascade-type dendrimer. Each spectrum is the smoothed average of three data sets.

ence of β-strands when compared with the spectrum of the pennant-type dendrimer at the same temperature. This is possibly due to the nature of the cascade-type dendrimer or the multiple β-strand branches present in the oxidized polymer compared to a monomeric pennant-type dendrimer.

Ice-binding and thermal hysteresis activity

To determine the dendrimer's ability to interact with an ice crystal surface it was necessary to use an organic solvent that in aqueous solution dissolved the peptide and did not interfere with ice-crystal morphology or thermal hysteresis activity (data not shown). A solution of acetic acid (9 %) and ACN (2 %) in 100 mM ammonium bicarbonate was selected as it did not alter ice-crystal morphology in a buffer control sample, see Figure 5. All TH activity readings were carried out in this buffer.

The ice crystal morphology produced by the pennant-type polypeptide as a monomer compared to solvent alone and a solution of *Cf*AFP isoform 501 is presented in Figure 5a. The solvent chosen produced a flat circular ice-crystal that increased in size upon cooling and decreased in size upon warming, as expected. The *Cf*AFP sample produced a characteristic hexagonal-shaped ice-crystal due to AFP binding to the primary prism and basal planes of ice. Generally, when an ice crystal forms in the presence of *Cf*AFP, it floats with its c-axis vertical but sometimes lies down as it lengthens along the c-axis. The crystal holds its shape and size while the temperature is decreased up to the crystal 'burst' point, see below. The ice crystal in the presence of the dendrimer polypeptide has flat hexagonal character suggesting binding of the polypeptide to specific planes of the ice-crystal. The ice crystal shape holds for over 30 minutes, which is not seen for solvent samples alone, suggesting that the polypeptide is binding to and stabilizing the ice crystal.

Thermal hysteresis activity is a property of antifreeze proteins and is described as the difference between the melting point and the non-equilibrium freezing point of a sample. This difference emerges in the presence of an antifreeze protein via binding of the protein to an ice crystal surface, thereby preventing more ice from forming on the seed crystal. When the cooling of a sample overcomes the adsorption inhibition effect of an AFP it can no longer protect the crystal and rapid ice growth or a "burst" is observed. The difference in the melting point and non-equilibrium freezing point is expressed in milliOsmoles (1000 mOsm = 1.86 oC) and is dependent on AFP concentration.

The monomeric dendrimer was able to bind to and stabilize an ice crystal but did not have any thermal hysteresis activity. The oxidized dendrimer dimer did show weak thermal hysteresis activity (0.09 C° at a concentration of 10 mg/ml.). The most active polypeptide was the oxidized polymer of three pennant-type dendrimers bound to one cascade-type dendrimer. A plot of thermal hysteresis activity as a function of polypeptide concentration is shown for the oxidized polymer of the dendrimer in Figure 5a. The polymer showed a maximum thermal hysteresis activity of around 185

mOsm or 0.34 Cº at a concentration of 15 mg/ml. The influence of the pH on the thermal hysteresis of the peptide was analyzed. A plot of thermal hysteresis activity vs. pH for the oxidized polymer at 10 mg/mL is presented as an insert in Figure 5a.

Examples of the 'bursts' produced by solvent alone, the oxidized dendrimer polymer and CfAFP isoform 501 are displayed in Figure 5b. The gradual circular growth of a circular ice crystal is observed for the solvent control illustrating that the acetic acid and ACN added

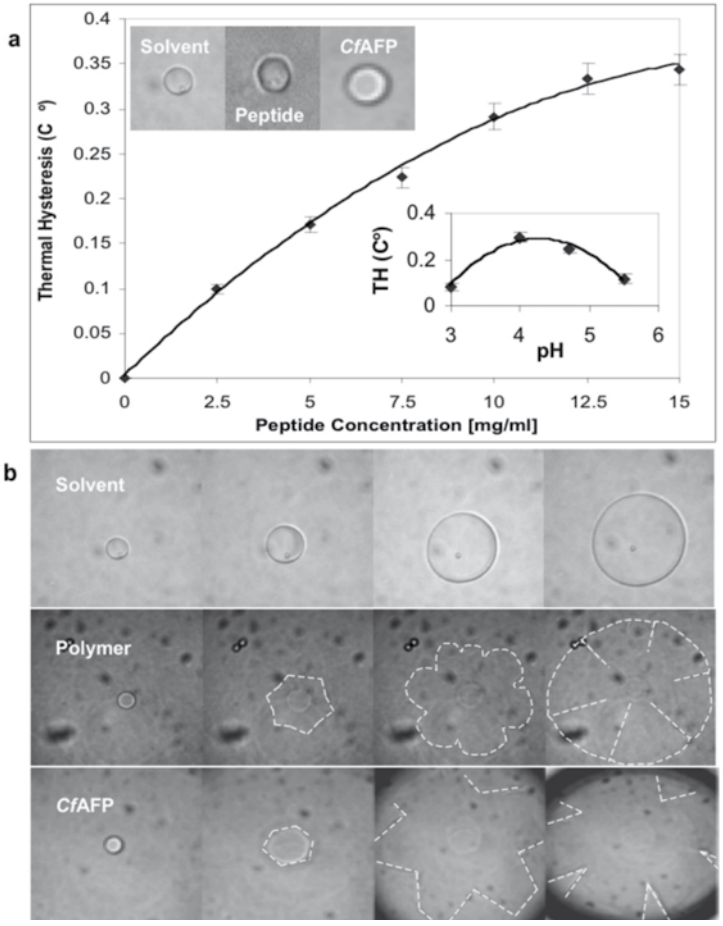

Figure 5. Effect of the dendrimer peptide on ice crystal morphology and growth. **a**. Thermal hysteresis activity as a function of dendrimer concentration. Inserts: lower right plot of pH Vs TH (10 mg/mL polymer); upper left morphology of the crystal without peptide, with peptide (10 mg/mL) and with *Cf*AFP isoform 501 (0.075 mg/mL). **b**. Ice crystal growth in solvent and a comparison of the ice crystal 'burst' in the presence of the synthetic polymeric antifreeze peptide (10 mg/mL) or *Cf*AFP isoform 501 (0.075 mg/mL). The white dotted lines indicate the extent and shape of the ice front after the rapid growth that characterizes the end of thermal hystereis.

to the buffer to dissolve the peptides do not alter typical ice crystal morphology. The oxidized polymer burst resembles a flower as the crystal bursts out from the six a-axes of the ice crystal. This burst is very similar to that observed for a sample of *Cf*AFP which also shows a hexagonal flower-like burst (44-45). This burst pattern is a characteristic of insect AFPs and those that bind to both the prism and basal planes of ice crystals (45). Not surprisingly, the oxidized dendrimer dimer and oxidized dendrimer polymer showed ice recrystallization inhibition activity at concentrations of 10 mg/mL (data not shown). Positive controls containing *Cf*AFP isoform 501 produced similar results. Recrystallization inhibition is another classical activity of ice-binding and antifreeze proteins whereby ice crystals in a flash frozen sample normally reorganize from multiple small crystals to fewer larger crystals as the sample approaches its melting point (46).

DISCUSSION

Here we show the design, synthesis and characterization of a pennant-type dendrimer polypeptide with functional branches based on the spruce budworm (*Choristoneura fumiferana*) and beetle (*Tenebrio molitor*) antifreeze proteins. A divergent, solid-phase, Fmoc chemistry-based synthetic strategy was employed to produce a pennant-type polypeptide composed of a backbone α-helix with four branching lysine residues. Short arms containing multiple repeats of a TXT motif from the ice-binding face of *Cf*AFP were synthesized at each branching point resulting in an array of potential ice-binding motifs protruding from one face of the α-helical backbone. These TXT arrays are presumably capable of forming multiple, simultaneous, interactions with a nascent ice crystal surface, consistent with morphological changes in the growing ice crystal that produced a flat hexagonal shape, similar to the crystal morphology produced by native insect AFPs (45).

Glycine residues were inserted at the beginning of each branch sequence to promote independent mobility of each branch and allow them to reorganize at the water-ice interface so that a good spatial distribution of the TXTXTXT motifs could be obtained. This was designed to improve the interaction between the threonine residues and the surface of the growing ice crystal. The ice binding face of *Cf*AFP is constituted of TXT motifs forming two parallel rows of threonine residues with spacing closely matching that of the basal plane and the prism planes of hexagonal ice crystals (19). The spacing between threonines in neighbouring TXT motifs makes an ideal match to the 4.5 Å distance between oxygen atoms along the *a*-axis in both the prism and basal planes of ice. At right angles to this repeat, the distance between threonines in the TXT motifs makes an ideal match to the 7.35 Å spacing of oxygen atoms on the prism plane. There is also a reasonable match to the 7.8 Å spacing of oxygen atoms on the basal plane. The pennant-type dendrimer polypeptide branches can mimic the 7.35 Å prism plane spacing and 7.8 Å basal plane spacing. In addition, the longer TXTXTXT repeats allow for an increased match to the prism plane via multiplication of the 7.35 Å spacing. The distance between branching point

Lys α-C residues varies between 6 - 6.5 Å for $K^4 – K^8$ and $K^{11} – K^{15}$ and is around 4.8 – 5.0 Å for $K^8 – K^{11}$. This does not quite match the 4.5 Å spacing in insect AFPs between Thr side-chains in the two linear arrays. However, the glycine residues at each branch point do allow for significant flexibility in the branches, so there could possibly be a match to the 4.5 Å prism plane spacing of water molecules in ice (or a multiple thereof) between two or more of the TXTXTXT repeats.

The synthetic polypeptide was indeed able to interact with ice crystals and alter their morphology in a similar manner to insect AFPs. A hexagonal shaped crystal was produced that is akin to the ice crystal morphology produced by solutions containing *Cf*AFP more so than that produced by *Tm*AFP. The *Tm*AFP ice-binding motif is also comprised of TXT repeats but these are arrayed on a disulfide bonded right-handed β-helix rather than a left-handed β-helix, although the spacing between threonine side-chains is very similar in both structures (47). The lack of a close 4.5 Å distance mimic did not prevent the monomeric pennant-type dendrimer polypeptide from binding to ice and altering its morphology, presumably through interactions at the prism and basal planes.

The monomeric dendrimer was not able to prevent the growth of an ice crystal as the temperature was decreased i.e. it did not possess thermal hysteresis activity. Oxidation of the monomer to form a disulfide bonded dimer with eight TXTXTXT branches produced a polypeptide that could bind to and inhibit the growth of ice crystals. The activity achieved was low compared to a native AFP (0.09 C° at 10 mg/mL). Further polymerization of the monomeric dendrimer with a trifunctional cascade dendrimer by oxidation produced a disulfide bonded trimer containing twelve TXTXTXT repeats with much higher thermal hysteresis activity than the dimer. A maximum activity of 0.34 C° at 10 mg/mL was recorded, again well below that expected for a native insect AFP but remarkable for a synthetic polypeptide. The big jump (four-fold) in thermal hysteresis activity on going from eight to twelve repeats is reminiscent of what is seen with insect AFPs when the number of TXT motifs is increased slightly. There is a four-fold increase in activity on going from five to six ice-binding coils in *Tm*AFP and a further two-fold increase on going from six to eight ice-binding coils (24). A two coil expansion in *Cf*AFP produced a three-fold increase in thermal hysteresis activity (23).

The optimum thermal hysteresis activity of the polymer was seen at a pH of 4.2. This result may be related to the structural stability of the peptide when the pH is acidic. This statement is supported by previous studies (48-49) that demonstrate some α-helical peptides show greater structural stability at acidic pH. This behavior has been attributed to negatively charged residues in α-helical sequences stabilizing the structure.

This polymer was also capable of inhibiting ice recrystallization at a concentration of 10 mg/mL. Although the concentration at which an end point was given was not determined it is safe to assume this would be much higher than that obtained for *Tm*AFP and *Cf*AFP.

Despite a complex design process, a divergent approach to solid-phase chemical synthesis produced a pennant-type dendrimer polypeptide with the expected molecular weight and secondary structural elements that are in agreement with theoretical predictions. Difficulties with some coupling and deprotection steps reduced the overall yield to 40% but this is quite respectable over so many couplings. The chosen strategy did allow for the synthesis of a complicated branched dendrimer that when oxidized or polymerized with a trifunctional cascade dendrimer showed thermal hysteresis and ice recrystallization inhibition activity akin to that of the native AFP (*Cf*AFP) that inspired the sequence of the branches. This approach based on dendrimer polypeptides highlights new possibilities for the design and generation of synthetic molecules with antifreeze activity that may have not only research value but also industrial and biomedical applications.

ACKNOWLEDGEMENTS

We thank Fundación Instituto de Inmunologia de Colombia, directed by Dr Manuel Elkin Patarroyo for the use of their facilities for peptide synthesis. We are grateful to Dr. Virginia Walker of the Biology Department at Queen's University, Kingston, Ontario, Canada for the help with ice recrystallization inhibition assays. We also thank Dr. Carmen M. Romero of the University National of Colombia for her assistance with the project. This work was partially supported by a Doctoral Fellowship from Instituto Colombiano para el Desarrollo de la Ciencia y la Tecnología Francisco José de Caldas (Colciencias) to RVB and by a grant from the Canadian Institutes for Health Research to PLD.

REFERENCES

1. Niederhafner P.; Sebestik J.; Jezek J. Peptide dendrimers. J. Pept. Sci. 2005. **11**:757-788.

2. Sadler K., Tam J.P. Peptide dendrimers: applications and synthesis. J. Biotechnol. 2002. **90**:195-229.

3. Tam J. P. 1996. Recent advances in multiple antigen peptides. J. Immunol. Methods. 196:17-32.

4. Tam, J.P. Synthesis and applications of branched peptides in immunologicalmethods and vaccines. In Peptides: Synthesis, Structures, and Applications. New York. Gutte, B., editors. Academic Press, 1995. pp. 455-500.

5. Tam J.P.; Spetzler J.C. Chemoselective approaches to the preparation of peptide dendrimers and branched artificial proteins using unprotected peptides as building blocks. Biomed. Pept. Proteins Nucleic Acids. 1995. **1**:123-132.

6. Tam J. P. Ligation and splicing of peptides and proteins. Biopolymers. 1999. **51**:309-310.

7. Tuchscherer G.; Servis C.; Corradin G.; Blum U.; Rivier J. Mutter M. Total chemical synthesis, characterization, and immunological properties of an MHC class I model using the TASP concept for protein de novo design. Protein Sci. 1992. **1**:1377-1386.

8. Al-Jamal K.T.; Ramaswamy C.; Florence. A.T. Supramolecular structures from dendrons and dendrimers. Adv. Drug. Deliv. Rev. 2005. **57**:2238-2270.

9. Kim Y.; Zimmerman S. C. Applications of dendrimers in bio-organic chemistry. Curr. Opin. Chem. Biol. 1998. **2**:733-742.

10. Cloninger M.J. Biological applications of dendrimers. Curr. Opin. Chem. Biol. 2002. **6**:742-748.

11. Lee C.C.; MacKay J.A.; Frechet J. M.; Szoka F.C. Designing dendrimers for biological applications. Nat. Biotechnol. 2005. **23**:1517-1526.

12. Bayley H. Designed membrane channels and pores. Curr. Opin. Biotechnol. 1999. **10**:94-103.

13. Hahn K.W.; Klis W.A.; Stewart J. M. Design and synthesis of a peptide having chymotrypsin-like esterase activity. Science. 1990. **248**:1544-1547.

14. Sasaki T.; Kaiser E.T. Synthesis and structural stability of helichrome as an artificial hemeproteins. Biopolymers. 1990. **29**:79-88.

15. Hauert J.; Fernandez-Carneado J.; Michielin O.; Mathieu S.; Grell D.; Schapira M.; Spertini O.; Mutter M.; Tuchscherer G.; Kovacsovics T. A template-assembled synthetic protein surface mimetic of the von Willebrand factor A1 domain inhibits botrocetin-induced platelet aggregation. Chembiochem. 2004. **5**:856-864.

16. Tuchscherer G.; Grell D.; Mathieu M.; Mutter M. Extending the concept of template-assembled synthetic proteins. J. Pept. Res. 1999. **54**:185-194.

17. Raymond J.A.; DeVries A.L. Adsorption inhibition as a mechanism of freezing resistance in polar fishes. Proc. Natl. Acad. Sci. USA. 1977. **74**:2589-2593.

18. Graether S.P.; Sykes B.D. Cold survival in freeze-intolerant insects: the structure and function of beta-helical antifreeze proteins. Eur. J. Biochem. 2004. **271**:3285-3296.

19. Graether S.P.; Kuiper M.J.; Gagne S.M.; Walker V.K.; Jia Z.; Sykes B.D.; Davies P.L. Beta-helix structure and ice-binding properties of a hyperactive antifreeze protein from an insect. Nature. 2000. **406**:325-328.

20. Marshall C.B.; Daley M.E.; Graham L.A.; Sykes B.D.; Davies P.L. Identification of the ice-binding face of antifreeze protein from Tenebrio molitor. FEBS Lett. 2002. **529**:261-267.

21. Doucet D.; Tyshenko M.G.; Kuiper M.J.; Graether S.P.; Sykes B.D.; Daugulis A.J.; Davies P.L.; Walker V.K. Structure-function relationships in spruce budworm antifreeze protein revealed by isoform diversity. Eur. J. Biochem. 2000. **267**:6082-6088.

22. Doucet D.; Tyshenko M.G.; Davies P.L.; Walker V.K. A family of expressed antifreeze protein genes from the moth, Choristoneura fumiferana. Eur. J. Biochem. 2002. **269**:38-46.

23. Leinala E.K.; Davies P.L.; Jia Z. Crystal structure of beta-helical antifreeze protein points to a general ice binding model. Structure. 2002. **10**:619-627.

24. Marshall C.B.; Daley M.E.; Sykes B.D.; Davies P.L. Enhancing the activity of a beta-helical antifreeze protein by the engineered addition of coils. Biochemistry. 2004. **43**:11637-11646.

25. Sarin V.K.; Kent S.B.; Tam J.P.; Merrifield R.B. Quantitative monitoring of solid-phase peptide synthesis by the ninhydrin reaction. Anal. Biochem. 1981. **117**:147-157.

26. Bycroft B.W.; Chan W.C.; Chhabra S.R.; Hone N.D. A novel lysine protecting procedure for continuous flow solid phase synthesis of branched peptides. J. Chem. Soc. Chem. Commun. 1993. **9**:778–779.

27. Combet C.; Blanchet C.; Geourjon C.; Deleage G. NPS@: network protein sequence analysis. Trends Biochem. Sci. 2000. **25**:147-150.

28. Chakrabartty A.; Yang D.S.; Hew C.L. Structure-function relationship in a winter flounder antifreeze polypeptide. II. Alteration of the component growth rates of ice by synthetic antifreeze polypeptides. J. Biol. Chem. 1989. **264**:11313-11316.

29. Walker V.K.; Palmer G.R.; Voordouw G. Freeze-thaw tolerance and clues to the winter survival of a soil community. Appl Environ Microbiol. 2006. **72**:1784-1792.

30. O'Neil K.T.; DeGrado W.F. A thermodynamic scale for the helix-forming tendencies of the commonly occurring amino acids. Science. 1990. **250**:646-651.

31. Koehl P.; Levitt M. Structure-based conformational preferences of amino acids. Proc. Natl. Acad. Sci. U S A. 1999. **96**:12524-12529.

32. Garnier J.; Osguthorpe D.J.; Robson B. Analysis of the accuracy and implications of simple methods for predicting the secondary structure of globular proteins. J. Mol. Biol. 1978. **120**:97-120.

33. Gibrat J.F.; Garnier J.; Robson B. Further developments of protein secondary structure prediction using information theory. New parameters and consideration of residue pairs. J. Mol. Biol. 1987. **198**:425-443.

34. Guermeur Y.; Geourjon C.; Gallinari P.; Deleage G. Improved performance in protein secondary structure prediction by inhomogeneous score combination. Bioinformatics. 1999. **15**:413-421.

35. Guermeur, Y. Combinaison de classifieurs statistiques, application a la prediction de structure secodarie des proteins. Ph. D. thesis, Pole Bioinformatique Lyonnais Network protein Sequence Analysis. 1997.

36. Rost B.; Sander C. Prediction of protein secondary structure at better than 70% accuracy. J. Mol. Biol. 1993. **232**:584-599.

37. Tam J.P. Synthetic peptide vaccine design-synthesis and properties of a high-density multiple antigenic peptide system. Proc. Natl. Acad. Sci. USA. 1988. **85**:5409-5413.

38. Manavalan P. and Johnson W.C. Sensitivity of circular dichroism to protein tertiary structure class. Nature. 1983. **305**:831-832.

39. Nordmann A.; Blommers M.J.; Fretz H.; Arvinte T.; Drake A.F. Aspects of the molecular structure and dynamics of neuropeptide Y. Eur. J. Biochem. 1999. **261**:216-226.

40. Li S.C.; Goto N.K.; Williams K.A.; Deber C.M. Alpha-helical, but not beta-sheet, propensity of proline is determined by peptide environment. Proc. Natl. Acad. Sci. USA. 1996. **93**:6676-6681.

41. Benaki D.C.; Mikros E.; Hamodrakas S.J. Conformational analysis of peptide analogues of silkmoth chorion protein segments using CD, NMR and molecular modelling. J. Pept. Sci. 2004. **10**:381-392.

42. Povey J.F.; Smales C.M.; Hassard S.J.; Howard M. J. Comparison of the effects of 2,2,2-trifluoroethanol on peptide and protein structure and function. J. Struct. Biol. 2007. **157**:329-338.

43. Roccatano D.; Colombo G.; Fioroni M.; Mark A.E. Mechanism by which 2,2,2-trifluoroethanol/water mixtures stabilize secondary-structure formation in peptides: a molecular dynamics study. Proc. Natl. Acad. Sci. USA. 2002. **99**:12179-12184.

44. Graham L.A.; Liou Y.C.; Walker V.K.; Davies P.L. Hyperactive antifreeze protein from beetles. Nature. 1997. **388**:727-728.

45. Scotter A.J.; Marshall C.B.; Graham L.A.; Gilbert J.A.; Garnham C.P.; Davies P.L. The basis for hyperactivity of antifreeze proteins. Cryobiology. 2006. **53**:229-239.

46. Knight C. A. and Duman J.G. Inhibition of recrystallization of ice by insect thermal hysteresis proteins: A possible cryoprotective role. Criobiology. 1986. 23:256-262.

47. Liou Y.C.; Tocilj A.; Davies P.L.; Jia Z. Mimicry of ice structure by surface hydroxyls and water of a beta-helix antifreeze protein. Nature. 2000. **406**:322-324.

48. Shoemaker K.R.; Kim P.S.; Brems D.N.; Marqusee S.; York E.J.; Chaiken I.M.; Stewart J.M.; Baldwin R.L. Nature of the charged-group effect on the stability of the C-peptide helix. Proc Natl Acad Sci USA. 1985. **82**:2349-2353.

49. Yaworsky D.C.; Baker B.Y.; Bose H.S.; Best K.B.; Jensen L.B.; Bell J.D.; Baldwin M.A.; Miller W. L. pH-dependent Interactions of the carboxyl-terminal helix of steroidogenic acute regulatory protein with synthetic membranes. J. Biol. Chem. 2005. **280**:2045-2054.